

A variational framework combining level-sets and thresholding.

Samuel Dambreville, Marc Niethammer, Anthony Yezzi
and Allen Tannenbaum
School of Electrical and Computer Engineering
Georgia Institute of Technology

Abstract

Segmentation involves separating distinct regions in an image. In this note, we present a novel variational approach to perform this task within the level-sets framework. We propose an energy functional that naturally combines two segmentation techniques usually applied separately: intensity thresholding and geometric active contours. Although our method can deal with more complex statistics, we assume that the pixel intensities of the regions have Gaussian distributions, in this work. The proposed approach affords interesting properties that can lead to sensible segmentation results.

1 Introduction

Segmentation involves separating an image into distinct regions, a ubiquitous task in computer vision applications. Active contours and image thresholding are among the most important techniques for performing this task.

Geometric active contour (GAC) can easily be combined with level-set methods in which a closed curve is represented implicitly as the zero level-set of a higher dimensional function (usually a signed distance function [11]). The curve is evolved to minimize a well-chosen energy functional, typically via gradient descent (see e.g., [11, 7, 6]). The implicit representation allows the curve to naturally undergo topological changes, such as splitting and merging. Different models have been proposed to perform segmentation with GACs: Some frameworks use local image features such as edges [12, 3], whereas other methods use regional image information such as intensity statistics, color or texture [13, 1, 4, 10]. Region based approaches usually offer a higher level of robustness to noise than techniques based on local information. Many of the region-based models have been inspired by the region competition technique proposed in [15]. The book [5] is a nice general reference on the various variational segmentation methods. In region-based frameworks, the intensity statistics of the image are estimated from the segmenting curve using parametric [1, 13, 10] or non-parametric [4] methods. While nonparametric approaches allow to deal with a wide class of images, parametric methods usually result in simple, robust and efficient segmentation algorithms.

In this note, we propose a novel region-based segmentation technique with GACs. Although the proposed method is general enough to deal with diverse image statistics, we only use intensity average and variance to separate regions, in this work. Hence, our

approach is close to the parametric technique proposed in [10]. However, the way image statistics are used in our framework is different and the resulting flow exhibits distinctive properties. We define a smooth energy functional that allows to employ the result of thresholding the image in order to evolve the contour.

The literature about image thresholding is large, and a complete survey is beyond the scope of this paper. The book [2] offers a nice introduction to classical techniques about this approach. Even if a simple thresholding method is used in this work, the power of the method emanates from the combination with GACs that can naturally split or merge as well as focus on a localized portion of the image.

In what follows, we first present our method and resulting flow. Then, we report experiments, which elucidate some key aspects of this method.

2 Proposed approach: GAC and Thresholding

We consider the problem of segmenting an image $I : \Omega \mapsto \mathcal{I}$, with $\Omega \subset \mathbf{R}^2$ and \mathcal{I} the space of possible intensity values (grey-scale). Let $x \in \Omega$ specify the coordinates of the pixels in the image I . Following [10], we assume that I is composed of two (unknown) homogeneous regions, referred to as ‘‘Object’’ and ‘‘Background’’, that have Gaussian distributions. We further assume that these regions have distinct variances¹. The goal of segmentation is to capture these two regions. To do so, we evolve a closed curve C , represented as the zero level-set of a signed distance function $\phi : \Omega \mapsto \mathbf{R}$, such that $\phi > 0$ inside C and $\phi < 0$ outside C . Our goal is to evolve the contour C , or equivalently ϕ , so that its interior matches the Object, and its exterior matches the Background: the curve C would then match the boundary separating Object and Background.

Let us denote by $H : \mathbf{R} \mapsto \{0, 1\}$ the Heaviside step function. A smooth version of H , denoted $H_\varepsilon : \mathbf{R} \mapsto [0, 1]$, can be computed as follows for a chosen parameter ε :

$$H_\varepsilon(\chi) = \begin{cases} = 1 & \text{if } \chi > \varepsilon ; \\ = 0 & \text{if } \chi < -\varepsilon ; \\ = \frac{1}{2} \{1 + \frac{\chi}{\varepsilon} + \frac{1}{\pi} \sin(\frac{\pi\chi}{\varepsilon})\} & \text{otherwise.} \end{cases} \quad (1)$$

The derivative of H_ε will be denoted by δ_ε ($\delta_\varepsilon(\chi) = 0$ if $|\chi| > \varepsilon$; and $\delta_\varepsilon(\chi) = \frac{1}{2\varepsilon} \{1 + \cos(\frac{\pi\chi}{\varepsilon})\}$ otherwise). In this note, a region $\mathcal{R} \subset \Omega$ is characterized by a smooth labeling function $R_\mathcal{R} : \Omega \mapsto [0, 1]$ such as $R_\mathcal{R}(x) \geq \frac{1}{2}$ if $x \in \mathcal{R}$ and $R_\mathcal{R}(x) < \frac{1}{2}$ if $x \in \Omega \setminus \mathcal{R}$. Thus, the segmentation defined by the interior of the contour C is characterized by the labeling function $H_{\varepsilon_1} \phi$.²

The intensity averages of the pixels located inside and outside the curve C , denoted by μ_{in} and μ_{out} respectively, can be computed *at each iteration of the evolution* as

$$\mu_{\text{in}} = \frac{\int_{\Omega} I(x) H\phi(x) dx}{A_{\text{in}}} \quad \text{and} \quad \mu_{\text{out}} = \frac{\int_{\Omega} I(x) (1 - H\phi(x)) dx}{A_{\text{out}}}, \quad (2)$$

where $A_{\text{in}} = \int_{\Omega} H\phi(x) dx$ and $A_{\text{out}} = \int_{\Omega} (1 - H\phi(x)) dx$ denote the areas inside and outside the curve, respectively. Similarly the variances inside (σ_{in}^2) and outside (σ_{out}^2) the

¹This is generally always the case in practice for a wide range of real-world images.

²For a chosen (small) ε_1 . In the remainder, we will often omit ε_1 in the expressions of $H_{\varepsilon_1} \phi$, and $\delta_{\varepsilon_1} \phi$, and denote $H\phi$ and $\delta\phi$ to simplify notation.

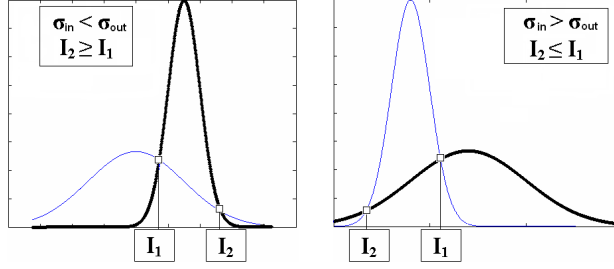


Figure 1: Probability density functions. Thick line: $P_{\text{in}}(I)$; Thin line: $P_{\text{out}}(I)$. It is straightforward to see that $P_{\text{in}}(I) > P_{\text{out}}(I)$ for $I_1 \leq I \leq I_2$, when $\sigma_{\text{in}} < \sigma_{\text{out}}$ and for $I \geq I_1$ and $I \leq I_2$, when $\sigma_{\text{in}} > \sigma_{\text{out}}$.

curve are computed as

$$\sigma_{\text{in}}^2 = \frac{\int (I(x) - \mu_{\text{in}})^2 H\phi(x) dx}{A_{\text{in}}} \quad \text{and} \quad \sigma_{\text{out}}^2 = \frac{\int (I(x) - \mu_{\text{out}})^2 (1 - H\phi(x)) dx}{A_{\text{out}}}. \quad (3)$$

Provided a meaningful initialization of the curve, these statistics bear valuable information about the statistics of the Object and the Background. Intuitively, the intensity averages μ_{in} and μ_{out} are the best available estimates of the unknown intensity averages μ_{O} and μ_{B} , respectively. Similarly σ_{in} and σ_{out} are the best estimates of σ_{O} and σ_{B} , available at the current step of the contour evolution. We propose to use these two statistical moments to threshold the image, assuming the Gaussian distribution of pixels. From Figure 1, the (conditional) densities P_{in} and P_{out} , of the pixels belonging inside and outside the contour, respectively, are equal for two intensity values I_1 and I_2 . Following the assumption $\sigma_{\text{in}} \neq \sigma_{\text{out}}$, these values can be computed as

$$I_1 = \frac{\sigma_{\text{out}}^2 \cdot \mu_{\text{in}} - \sigma_{\text{in}}^2 \cdot \mu_{\text{out}} - \sigma_{\text{out}} \sigma_{\text{in}} \cdot \alpha}{\sigma_{\text{out}}^2 - \sigma_{\text{in}}^2} \quad \text{and} \quad I_2 = \frac{\sigma_{\text{out}}^2 \cdot \mu_{\text{in}} - \sigma_{\text{in}}^2 \cdot \mu_{\text{out}} + \sigma_{\text{out}} \sigma_{\text{in}} \cdot \alpha}{\sigma_{\text{out}}^2 - \sigma_{\text{in}}^2}, \quad \text{with} \quad (4)$$

$$\alpha = \sqrt{(\mu_{\text{in}} - \mu_{\text{out}})^2 + 2(\sigma_{\text{in}}^2 - \sigma_{\text{out}}^2) \log\left(\frac{\sigma_{\text{in}}}{\sigma_{\text{out}}}\right)}.$$

To perform the thresholding operation, we define the labeling function $G : \Omega \mapsto [0, 1]$ so that pixels x that are more likely to belong to the Object, i.e., $P_{\text{in}}(I(x)) \geq P_{\text{out}}(I(x))$, are assigned a value $G(x) \geq \frac{1}{2}$, whereas pixels more likely to belong to the Background, i.e., $P_{\text{in}}(I(x)) < P_{\text{out}}(I(x))$, are assigned a value $G(x) < \frac{1}{2}$. Based on Figure 1, a natural candidate for the function G is

$$\text{if } \sigma_{\text{in}} < \sigma_{\text{out}}, \quad G(x) = \begin{cases} \geq \frac{1}{2} & \text{if } I_2 \geq I(x) \geq I_1; \\ < \frac{1}{2} & \text{else.} \end{cases}$$

$$\text{if } \sigma_{\text{in}} > \sigma_{\text{out}}, \quad G(x) = \begin{cases} \geq \frac{1}{2} & \text{if } I(x) \geq I_1 \text{ or } I(x) < I_2; \\ < \frac{1}{2} & \text{else.} \end{cases}$$

Using the smooth version of the Heaviside function described above (for a chosen smooth-

ness parameter ε_2), the function G can be chosen to be³

$$G(x) = \begin{cases} H_{\varepsilon_2}(I(x) - I_1) - H_{\varepsilon_2}(I(x) - I_2) & \text{if } \sigma_{\text{in}} < \sigma_{\text{out}} ; \\ 1 + H_{\varepsilon_2}(I(x) - I_1) - H_{\varepsilon_2}(I(x) - I_2) & \text{if } \sigma_{\text{in}} > \sigma_{\text{out}} \end{cases} \quad (5)$$

To perform the segmentation, we propose to minimize

$$E_{\text{image}}(\phi, I) = \|H\phi - G\|^2 = \int_{\Omega} \{H\phi(x) - G(x)\}^2 dx. \quad (6)$$

This energy is the L_2 distance between the (*current*) segmentation $H\phi$ obtained from the curve C and the (*implied*) segmentation G obtained from thresholding the image I . The minimization is performed by evolving C according to the flow:

$$\frac{d\phi}{dt} = -\nabla_{\phi} E_{\text{image}} + \lambda \cdot \delta\phi \cdot \text{div} \left(\frac{\nabla\phi}{|\nabla\phi|} \right) \quad (7)$$

where the second term in the right-hand side is a regularizing term penalizing high curvatures (the parameter $\lambda \in \mathbf{R}^+$ is chosen subjectively). The gradient $\nabla_{\phi} E_{\text{image}}$ can be computed using calculus of variations (both $H\phi$ and G depend on ϕ):

$$\nabla_{\phi} E_{\text{image}} = 2\delta\phi(H\phi - G) + 2(\beta_1 \cdot \nabla_{\phi} I_1 - \beta_2 \cdot \nabla_{\phi} I_2) \quad (8)$$

where the expressions of $\beta_1 \in \mathbf{R}$ and $\beta_2 \in \mathbf{R}$ are

$$\beta_1 = \int_{\Omega} \delta_{\varepsilon_2}(I(x) - I_1) [H\phi(x) - G(x)] dx \quad \& \quad \beta_2 = \int_{\Omega} \delta_{\varepsilon_2}(I(x) - I_2) [H\phi(x) - G(x)] dx. \quad (9)$$

The expressions of $\nabla_{\phi} I_1$ and $\nabla_{\phi} I_2$ are detailed in the Appendix. The gradient $\nabla_{\phi} E_{\text{image}}$ is the sum of two terms. The first term, namely $2\delta\phi(H\phi - G)$, simply points towards G : Image pixels (in the vicinity of C), which are more likely to belong to the Object are included in C , whereas pixels more likely to belong to the Background are excluded. Hence, this term influences the contour based only on statistical considerations. As will be highlighted in the experimental part, this first term drives the contour in a similar fashion as the gradient proposed in [10], which also stems from statistical considerations of the intensity distributions only. The second term, namely $2(\beta_1 \cdot \nabla_{\phi} I_1 - \beta_2 \cdot \nabla_{\phi} I_2)$, involves the gradients of the thresholds I_1 and I_2 with respect to ϕ (which in turn involve $\nabla_{\phi} \mu_{\text{in}}$, $\nabla_{\phi} \mu_{\text{out}}$, $\nabla_{\phi} \sigma_{\text{in}}$ and $\nabla_{\phi} \sigma_{\text{out}}$; see Appendix). Such a term is not present in the flows presented in [1, 10]. Depending on the sign of β_1 (respectively, β_2), this second term points in the direction of the fastest increase or decrease of the threshold I_1 (respectively, I_2), resulting in changing G to decrease E_{image} . The coefficients β_1 and β_2 are essentially counting functions focusing on the ‘‘ambiguous pixels’’, i.e. pixels which intensities are close to the thresholds I_1 and I_2 (C.f. the terms $\delta(I - I_1)$ and $\delta(I - I_2)$, in the expressions of β_1 and β_2) and for which classification is the most uncertain. The sign and magnitude of β_1 and β_2 are conditioned upon the number of ambiguous pixels that belong to one of the segmentations ($H\phi$ or G) but not the other. To better understand the influence of this second term, we propose to consider the following example:

³In the limit case, when $\varepsilon_2 \rightarrow 0$, G is the result of *hard thresholding* the image I using the band(s) defined by I_1 and I_2 .

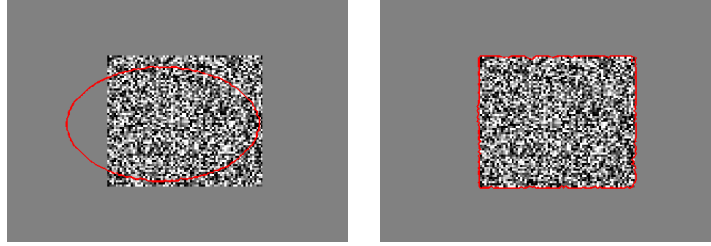


Figure 2: Synthetic Example, two regions of same mean intensity and different variances. *Left*: Initialization ; *Right*: Final segmentation.

Let us assume that ambiguous pixels with values close to I_1 are in majority outside the contour. The coefficient β_1 is thus negative. In the gradient descent process of Equation (7), the curve evolves in the direction of $\nabla_{\phi} I_1$, which increases I_1 . This results in excluding ambiguous pixels from the segmentation G leading to a better match with the segmentation defined by the curve.

Hence, the second term of $\nabla_{\phi} E_{\text{image}}$ appears to make meaningful decisions of the type: if more ambiguous pixels are inside C (resp. outside) then take more ambiguous pixels inside G (resp. outside). This systematic treatment of the thresholds I_1 and I_2 afforded by the second term of $\nabla_{\phi} E_{\text{image}}$ is an important feature of this work, and will be further examined in the experimental part below.

3 Experimental Results

We now present experimental results, typically using the heuristic $\varepsilon_2 = 3 \times \varepsilon_1$ for gray-scale images $I : \Omega \mapsto \{0..255\}$. The parameter λ was chosen subjectively in $[0, 2]$.

In Figure 2, a synthetic image composed of two regions that have the same average intensities and different variances is successfully segmented with our method.

In Figure 3, two textured natural images are segmented. The segmentation of the leopard obtained with our method is convincing compared to the segmentation obtained in [4], where the mutual information between general distributions of pixel intensities was minimized. The zebra is also successfully segmented even though only the average and variance of pixel intensities are used (This image was segmented before using more involved image information, such as texture [8] or general pixel distribution [4, 9]).

Segmenting medical images is usually a challenging task, since structures of interest are often poorly contrasted with respect to other neighboring structures. The proposed method was found to perform in a satisfactory manner on such images. In what follows, we report three experiments and contrast our results with results obtained using the method proposed in [10] that uses the same image information (intensity averages and variances). In Figure 4, the hand of a patient with a Kaposi Sarcoma (KS) is segmented. The contour is initialized in the vicinity of the KS, and an acceptable segmentation of the pathology is obtained with our method (i.e., using the full expression of ∇E_{image} as in Equation (8)). Using the flow proposed in [10], for the same initialization, the contour ends up capturing the whole visible part of the hand. A similar result was obtained using the first term in ∇E_{image} only. In Figures 5 and 6, MRI images of the heart are segmented.

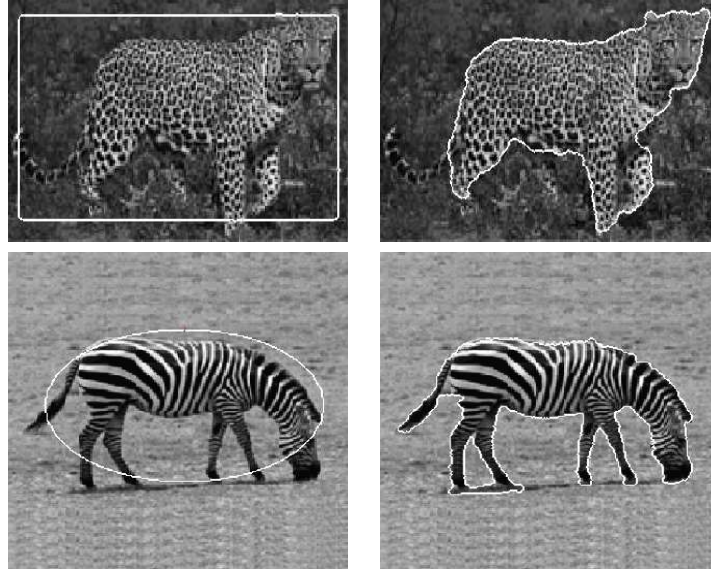


Figure 3: Segmentation results of two natural images. *Left*: Initialization, *Right*: Segmentation result with the proposed method.

Convincing segmentations of the left ventricle are obtained with our method (The results obtained were identical for a wide range of shapes of the initial contour). A comparable segmentation of the image in Figure 5 was obtained in [14], where global constraints were imposed on the flow presented in [13]. Using the method proposed in [10] or the first term of ∇E_{image} only, the ventricle is not properly segmented. In Figure 7, a transverse MRI-image of the brain is presented. The caudate nuclei are notoriously difficult to segment due to their poor contrast with neighboring structures. An acceptable segmentation of the left and right caudate is obtained with our method. Using the method proposed in [10] or the first term of ∇E_{image} only, the whole white and grey matter of the brain is segmented, even though the contour was initialized in the vicinity of the caudate nuclei.

Hence, in view of the experiments performed, our method appears to lead to meaningful segmentations notably in the case of medical images. When only the first term of ∇E_{image} is used, similar results as [10] were obtained. This highlights the influence of the second term in ∇E_{image} . This term evolves the contour in ways that modify G to match $H\phi$ as fast as possible (by changing the statistics inside and outside the curve). This can be further noticed from observing the final thresholded images in Figures 4 and 5, whether the second term of ∇E_{image} is used or not. Thus, the second term in ∇E_{image} has the advantageous effect of better exploiting some of the information built in the initial contour (e.g., placement, shape or size) and allows for the segmentation of objects/structures that are in its vicinity. Furthermore, these experiments suggest that using statistical information alone may not be enough to lead to meaningful segmentation results.

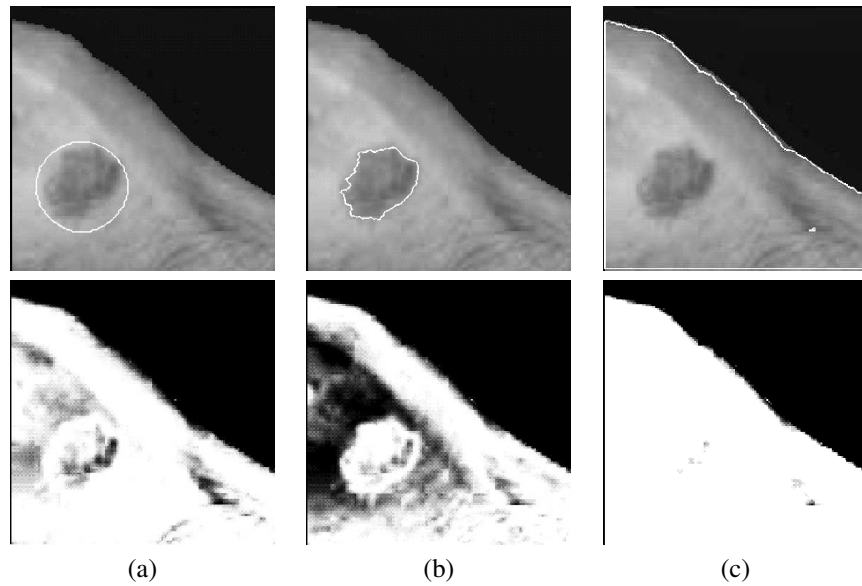


Figure 4: Segmentation of the hand of a patient with a Kaposi Sarcoma. *Top Row:* (a)-Initialization; (b)-Final segmentation with the proposed method; (c)-Final segmentation with the method proposed in [10] or with the first term of ∇E_{image} only. *Bottom Row:* Corresponding thresholded images.

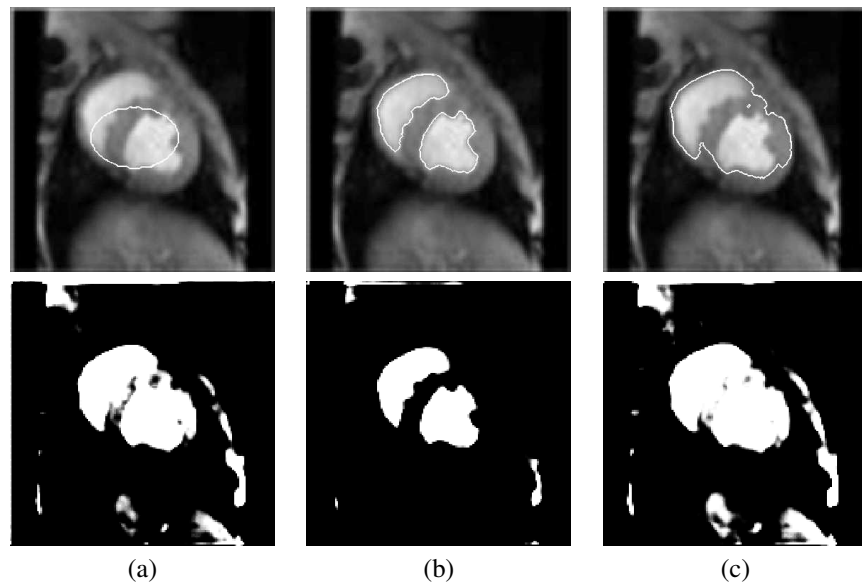


Figure 5: Segmentation of an MRI image of the heart. *Top Row:* (a)-Initialization; (b)-Final segmentation with the proposed method; (c)-Final segmentation with the method proposed in [10] or with the first term of ∇E_{image} only. *Bottom Row:* Corresponding thresholded images.

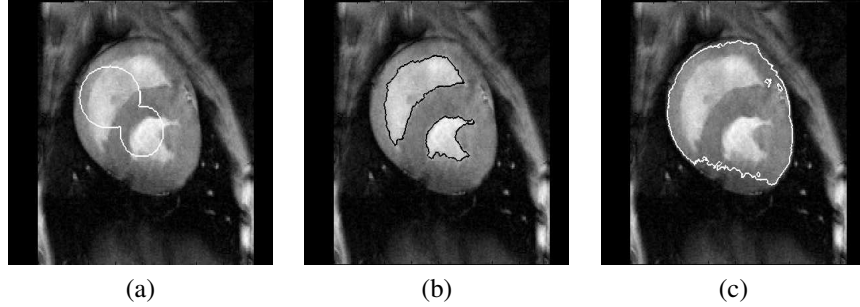


Figure 6: Other segmentation of an MRI image of the heart. (a)-Initialization; (b)-Final segmentation with the proposed method; (c)-Final segmentation with the method proposed in [10] or with the first term of ∇E_{image} only.

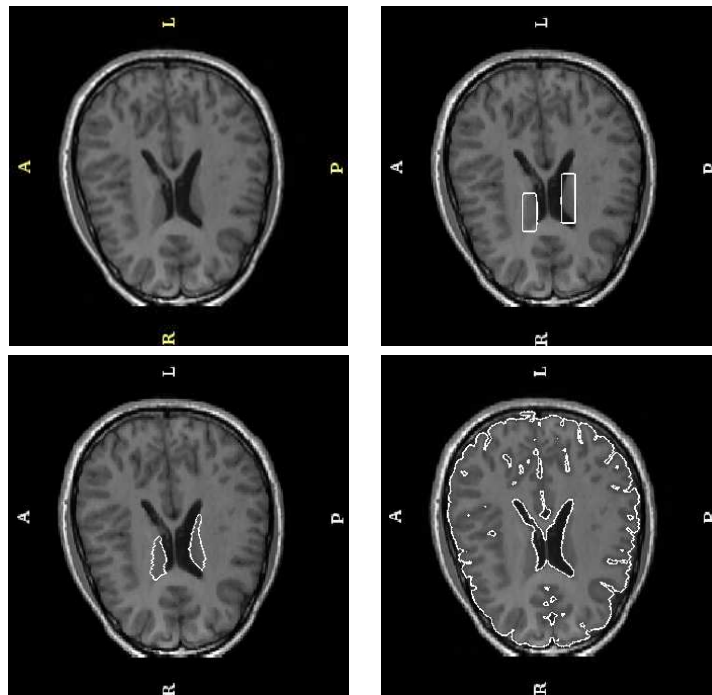


Figure 7: Segmentation of the caudate nuclei. *Top Left*: MRI image of the brain. *Top Right*: Contour initialization. *Bottom Left*: Final segmentation with the proposed method. *Bottom Right*: Final segmentation with the method proposed in [10] or with the first term of ∇E_{image} only.

4 Conclusions and Future Research

In this work, we presented a variational approach combining two segmentation techniques: active contours and thresholding. In the proposed framework, image statistics (intensity averages and variances) are exploited in a novel manner by defining an energy functional that compares the segmentation obtained from the evolving curve with the segmentation obtained from thresholding the image. Our region-based approach was shown to lead to convincing results on nontrivial real-world examples that were successfully segmented before, but using much more involved segmentation schemes. The proposed method also led to improved results for a variety of medical images in comparison with a previously proposed variational approach that uses the same statistical information. The flow resulting from our energy functional seems to afford some useful properties allowing the segmenting curve to reach local energy minima that coincide with meaningful segmentations. In our future work, we plan to expand the proposed approach to incorporate various image information such as intensity histograms or texture. The use and influence of different metrics to define our energy is also the interest of our future research.

References

- [1] T. Chan and L. Vese. Active contours without edges. *IEEE Trans. on Image Processing*, 10(2):266–277, 2001.
- [2] Rafael C. Gonzalez and Richard E. Woods. *Digital Image Processing*. Addison-Wesley Longman., 2001.
- [3] S. Kichenassamy, S. Kumar, P. Olver, A. Tannenbaum, and A. Yezzi. Conformal curvature flow: From phase transitions to active vision. In *Archives for Rational Mechanics and Analysis*, volume 134, pages 275–301, 1996.
- [4] J. Kim, J. Fisher, A. Yezzi, M. Cetin, and A. Willsky. Nonparametric methods for image segmentation using information theory and curve evolution. In *Proc. ICIP*, volume 3, pages 797–800, 2002.
- [5] J-M Morel and S. Solimini. *Variational Methods for Image Segmentation*. Birkhauser, 1994.
- [6] S. Osher and R. Fedkiw. *Level Set Methods and Dynamic Implicit Surfaces*. Springer Verlag, 2003.
- [7] N Paragios, Y. Chen, and O Faugeras. *Handbook of Mathematical Models in Computer Vision*. Springer, 2005.
- [8] N. Paragios and R. Deriche. Geodesic active regions for supervised texture segmentation. In *ICCV (2)*, pages 926–932, 1999.
- [9] Y. Rathi, O. Michailovich, and A. Tannenbaum. Seeing the unseen: Segmenting with distributions. In *Intl. Conf. Signal and Image Processing*, volume 534, 2006.
- [10] M. Rousson and R. Deriche. A variational framework for active and adaptative segmentation of vector valued images. In *Proc. of the Workshop on Motion and Video Computing*, page 56, 2002.

- [11] J. A. Sethian. *Level Set Methods and Fast Marching Methods*. 1999.
- [12] V.Caselles, R. Kimmel, and G. Sapiro. Geodesic active contours. In *IJCV*, volume 22, pages 61–79, 1997.
- [13] A. Yezzi, A. Tsai, and A. Willsky. A statistical approach to snakes for bimodal and trimodal imagery. In *Proc. ICCV*, volume 2, pages 898–903, 1999.
- [14] A. Yezzi, A. Tsai, and A. Willsky. Medical image segmentation via coupled curve evolution equations with global constraints. In *Proc. Workshop on Mathematical Methods in Biomedical Image Analysis*, pages 12–19, 2000.
- [15] Song Chun Zhu and Alan L. Yuille. Region competition: Unifying snakes, region growing, and Bayes/MDL for multiband image segmentation. volume 18, pages 884–900, 1996.

5 Appendix: Further details on the proposed flow

We now detail the expressions of $\nabla_\phi I_1$ and $\nabla_\phi I_2$, which appear in Equation (8). These expressions involve $\nabla_\phi \mu_{\text{in}}$, $\nabla_\phi \mu_{\text{out}}$, $\nabla_\phi \sigma_{\text{in}}$ and $\nabla_\phi \sigma_{\text{out}}$, which are given by

$$\begin{aligned} \nabla_\phi \mu_{\text{in}} &= \delta\phi \left(\frac{I - \mu_{\text{in}}}{A_{\text{in}}} \right) & , & & \nabla_\phi \mu_{\text{out}} &= \delta\phi \left(\frac{\mu_{\text{out}} - I}{A_{\text{out}}} \right) \\ \nabla_\phi \sigma_{\text{in}} &= \delta\phi \left(\frac{(I - \mu_{\text{in}})^2 - \sigma_{\text{in}}^2}{2\sigma_{\text{in}} \cdot A_{\text{in}}} \right) & \text{and} & & \nabla_\phi \sigma_{\text{out}} &= \delta\phi \left(\frac{\sigma_{\text{out}}^2 - (I - \mu_{\text{out}})^2}{2\sigma_{\text{out}} \cdot A_{\text{out}}} \right). \end{aligned} \quad (10)$$

From Equation (4) and using classical rules of calculus, one gets

$$\begin{aligned} \nabla_\phi I_1 &= m_1^{\text{in}} \cdot \nabla_\phi \mu_{\text{in}} + m_1^{\text{out}} \cdot \nabla_\phi \mu_{\text{out}} + s_1^{\text{in}} \cdot \nabla_\phi \sigma_{\text{in}} + s_1^{\text{out}} \cdot \nabla_\phi \sigma_{\text{out}}. \\ \nabla_\phi I_2 &= m_2^{\text{in}} \cdot \nabla_\phi \mu_{\text{in}} + m_2^{\text{out}} \cdot \nabla_\phi \mu_{\text{out}} + s_2^{\text{in}} \cdot \nabla_\phi \sigma_{\text{in}} + s_2^{\text{out}} \cdot \nabla_\phi \sigma_{\text{out}}. \end{aligned} \quad (11)$$

where the parameters m_1^{in} , m_1^{out} , s_1^{in} and s_1^{out} are

$$\begin{aligned} m_1^{\text{in}} &= \frac{1}{\sigma_{\text{out}}^2 - \sigma_{\text{in}}^2} \left(\sigma_{\text{out}}^2 - \sigma_{\text{in}} \sigma_{\text{out}} \left(\frac{\mu_{\text{in}} - \mu_{\text{out}}}{\alpha} \right) \right) \\ m_1^{\text{out}} &= \frac{1}{\sigma_{\text{out}}^2 - \sigma_{\text{in}}^2} \left(\sigma_{\text{in}} \sigma_{\text{out}} \left(\frac{\mu_{\text{in}} - \mu_{\text{out}}}{\alpha} \right) - \sigma_{\text{in}}^2 \right) \\ s_1^{\text{in}} &= \frac{1}{\sigma_{\text{out}}^2 - \sigma_{\text{in}}^2} \left\{ 2\sigma_{\text{in}} \sigma_{\text{out}} \left(\frac{\sigma_{\text{out}} \mu_{\text{in}} - \sigma_{\text{out}} \mu_{\text{out}} - \sigma_{\text{in}} \cdot \alpha}{\sigma_{\text{out}}^2 - \sigma_{\text{in}}^2} \right) - \right. \\ &\quad \left. \left(\sigma_{\text{out}} \cdot \alpha + \frac{2\sigma_{\text{in}}^2 \sigma_{\text{out}}}{\alpha} \log \left(\frac{\sigma_{\text{in}}}{\sigma_{\text{out}}} \right) + \sigma_{\text{out}} \frac{\sigma_{\text{in}}^2 - \sigma_{\text{out}}^2}{\alpha} \right) \right\} \\ s_1^{\text{out}} &= \frac{1}{\sigma_{\text{out}}^2 - \sigma_{\text{in}}^2} \left\{ 2\sigma_{\text{in}} \sigma_{\text{out}} \left(\frac{\sigma_{\text{in}} \mu_{\text{out}} - \sigma_{\text{in}} \mu_{\text{in}} + \sigma_{\text{out}} \cdot \alpha}{\sigma_{\text{out}}^2 - \sigma_{\text{in}}^2} \right) - \right. \\ &\quad \left. \left(\sigma_{\text{in}} \cdot \alpha - \frac{2\sigma_{\text{in}} \sigma_{\text{out}}^2}{\alpha} \log \left(\frac{\sigma_{\text{in}}}{\sigma_{\text{out}}} \right) - \sigma_{\text{in}} \frac{\sigma_{\text{in}}^2 - \sigma_{\text{out}}^2}{\alpha} \right) \right\} \end{aligned}$$

The expressions for the parameters m_2^{in} , m_2^{out} , s_2^{in} and s_2^{out} are identical to the expressions of m_1^{in} , m_1^{out} , s_1^{in} and s_1^{out} , replacing α by $-\alpha$.